Archean andesites in the east Yilgarn craton, Australia: Products of plume-crust interaction?

Stephen J. Barnes[1] and Martin J. Van Kranendonk[2,3]

[1]EARTH SCIENCE AND RESOURCE ENGINEERING, COMMONWEALTH SCIENTIFIC AND INDUSTRIAL RESEARCH ORGANISATION (CSIRO), KENSINGTON, PERTH, WESTERN AUSTRALIA 6151, AUSTRALIA

[2]SCHOOL OF BIOLOGICAL, EARTH AND ENVIRONMENTAL SCIENCES, UNIVERSITY OF NEW SOUTH WALES, KENSINGTON, NEW SOUTH WALES 2052, AUSTRALIA

[3]ARC CENTRE OF EXCELLENCE FOR CORE TO CRUST FLUID SYSTEMS, DEPARTMENT OF EARTH AND PLANETARY SCIENCES, MACQUARIE UNIVERSITY, NORTH RYDE, NEW SOUTH WALES 2109, AUSTRALIA

ABSTRACT

The timing of onset of modern plate tectonics on Earth is one of the fundamental unsolved problems in geology: How similar were the tectonic processes on early Earth, when the mantle was hotter and the crust more ductile, to those operating today? A key line of evidence for Archean (pre–2.7 Ga) plate tectonics rests on the presence of andesites, intermediate lavas that are the signature rock type of modern subduction zones. The 2.7 Ga Eastern Goldfields superterrane of the Yilgarn craton (herein east Yilgarn craton) in Western Australia is a richly mineral-endowed crustal element that has been a prime focus of debate between proponents of an uniformitarian, plate-tectonic–driven interpretation, and advocates of an alternative model wherein the entire assemblage of igneous rocks is derived ultimately from mantle plume activity. Andesites are a key component of the volcanic stratigraphy and potentially provide critical clues to the evolution of this piece of Archean lithosphere.

Whereas east Yilgarn craton andesites have incompatible trace-element characteristics similar to those of modern island-arc andesites, they are distinguished by unusually high Ni, Cr, and MgO contents. Numerical modeling of fractionation of plume-related tholeiitic basalts, coupled with contamination by contemporaneous partial melts of preexisting continental crust, provides a good fit to this feature, along with all of the essential major- and trace-element characteristics of the east Yilgarn craton andesites. Thus, a rock type previously taken as a key line of evidence for plate-tectonic processes in the east Yilgarn craton can be explained just as well by a plume-driven mechanism, which is more consistent with the overwhelmingly plume-derived character of basalts and komatiites across the entire craton. This explains a paradox noted in many pre–2.7 Ga volcanic rock sequences around the world, namely, that apparently subduction-related rocks are interleaved with voluminous basaltic magmatism derived from 1000-km-scale plume-head arrival events. The problem is moot if Archean andesites are products of plume, not subduction-zone, magmatism.

LITHOSPHERE; v. 6; no. 2; p. 80–92 doi: 10.1130/L356.1

INTRODUCTION

Much of the evidence for the operation of subduction on early Earth is based on the geochemistry of volcanic rocks found in Archean granite-greenstone terranes, particularly calc-alkaline andesites, which commonly bear striking geochemical similarities to their counterparts from Phanerozoic arc complexes (Barley et al., 2006b; Kositcin et al., 2007). The inferred uniformitarian growth mechanism for Archean crust through subduction-accretion is seemingly supported by evidence for convergent tectonics, terrane accretion, and presence of structural elements that are locally similar to modern active continental margins (Swager and Griffin, 1990; Blewett et al., 2010). However, Archean granite-greenstone terranes also show a number of features that are distinctly different from their proposed modern counterparts. Such features include: the widespread occurrence of komatiites; prevalence of basalts with strong geochemical similarities to modern oceanic plateau compositions; dominance of low-pressure over high-pressure metamorphism; almost exclusively submarine volcanism; lack of accretionary prisms and ophiolites; scarcity of true andesites; and development of late-stage "blooms" of vast volumes of tonalite-trondhjemite-granodiorite (TTG) granitoids (Hamilton, 1998; Bédard et al., 2013). This leads to something of a paradox: basaltic assemblages have chemical compositions that strongly suggest mantle plume derivation (Barnes et al., 2012), whereas the interbedded calc-alkaline intermediate-felsic complexes are interpreted to derive from convergent margin processes in the absence of plume input. One school of thought appeals to models of plume-arc interaction (Kerrich et al., 1998; Wyman et al., 2002), but the juxtaposition of widespread plume-derived volcanism—in the east Yilgarn case, over an area of more than 50,000 km^2—with localized subduction-zone magmatism (typically <1000 km^2) poses major problems of scale (e.g., Barnes et al., 2012). The local interlayering of plume and arc magmas, repeated up to four times in the Abitibi belt (Ayer et al., 2002), requires highly complex tectonic models (Bédard, 2013; Bédard et al., 2013).

A critical factor in this paradox is the origin of Archean andesites. Although Phanerozoic andesites overwhelmingly form at convergent margins as a result of subduction-derived melting, calc-alkaline intermediate rocks have also been recorded in ocean islands, oceanic plateaus, continental large igneous provinces, and back-arc spreading centers, albeit in very small proportions (Hooper et al., 2002; Scarrow et al., 2008; Willbold et al., 2009). Petrogenetic models for andesites in general commonly call on processes of mixing between mafic and felsic magmas, regardless of tectonic environment (Reubi and Blundy, 2009). For example, a non–subduction setting has been deduced from a detailed study of Paleoarchean andesites from the Pilbara craton in Western Australia, which concluded that their origin was a result of fractionation

of a large basaltic magma chamber combined with contamination by felsic crust (Smithies et al., 2007). Bédard et al. (2013) proposed that trace-element patterns of Archean andesites are consistent with this type of mixing process. In contrast, Morris and Kirkland (2014) propose a subduction related model for c. 2730 Ma old andesites in the central Yilgarn craton.

This contribution considers the compositions of 2.69–2.71 Ga andesites from the Eastern Goldfields superterrane of the Yilgarn craton (herein referred to as the east Yilgarn craton) in the context of the geochemical variability in the entire coeval volcanic suite, and in comparison with modern island-arc terranes. We examine the critical question of whether subduction is a necessary process in the petrogenesis of andesites, or whether plume-driven interpretations are equally plausible. Our results suggest that the volcanic assemblage of much of the east Yilgarn craton was a plume-related large igneous province, along the lines originally suggested by Campbell and Hill (1988), with the regional distribution of rock types being controlled by interaction of the source mantle plume with a preexisting Archean cratonic nucleus.

METHODS

The approach taken in this study was to compile all of the publicly available whole-rock geochemical data on volcanic and associated hypabyssal intrusive rocks from the greenstone belts of the east Yilgarn craton (see Table 1 for data sources) and to compare them with the large body of published analyses of Phanerozoic island-arc volcanic rocks from the extensive online GEOROC database (Sarbas, 2008). Data from the east Yilgarn craton are plotted over data density contours created using ioGAS™ software based on the GEOROC data set. Contours are shown for the intermediate to felsic component of the data set only, leaving out the basalts for clarity and also because of the uneven sampling probability for basalts relative to felsic volcanic rocks in arcs.

For the geochemical modeling, we considered a variety of possible mixing and assimilation models for the derivation of the east Yilgarn craton andesites from the coeval mafic and ultramafic parent magmas represented within the greenstone sequence. These models were carried out using the program PELE (Boudreau, 1999), an implementation of the MELTS thermodynamic simulation of silicate melt equilibria (Ghiorso and Sack, 1995). Assimilation models assumed addition of a liquid contaminant of the given composition, assuming simultaneous crystallization of the parent magma coupled with addition of a constant relative mass of contaminant at each crystallization step, calculated at ten degree intervals. Variable input parameters included (1) the relative rate of assimilation and crystallization; (2) pressure; (3) equilibrium versus fractional crystallization; and (4) whether or not spinel was included as a potential crystallizing phase. The assimilation-crystallization simulations modeled the process as a combination of equilibrium crystallization (i.e., with no mass transfer out of the system, and phases continuously equilibrating with one another as they form) and addition of molten dacite contaminant in a fixed proportion. Input compositions are discussed further later herein.

TABLE 1. DATA SOURCES FOR INTERMEDIATE TO FELSIC EAST YILGARN ROCKS

Locality	Reference	Easting	Northing	No. of samples
Abattoir	Barley et al. (2006a)			1
Albion Downs		248371	7001767	1
Albion Downs	CSIRO/UWA (pers. commun, 2012)	248550	7004300	9
Black Swan	Hill et al. (1999, 2004)	369428	6636850	63
Boundary–Dingo Range	Geoscience Australia (2007)	346000	6970000	4
Carnilya Hill	Said et al. (2010)	392261	4563224	3
Chesapeake	Barley et al. (2006a)	408072	6774325	2
Harmony	Duuring et al. (2007, 2010)	272600	6926000	6
Hootanni GA	Geoscience Australia (2007)	398000	6959000	3
Jundee-Nimary	Barley et al. (2006a)	263457	7069197	4
Kalgoorlie	Barley et al. (2006a)	356763	6588201	1
Kalgoorlie	Beresford et al. (2004); Said et al. (2010)	357870	6590700	1
Kambalda unspecified	Barley et al. 2006a)	360555	6583373	16
Karonie N	Barley et al. (2006a)	454616	6576933	1
Lady Edith	Barley et al. (2006a)	447061	6743583	2
Lancefield-Windarra	Geoscience Australia (2007)	426000	6845000	2
Laverton GA	Geoscience Australia (2007)	447000	6822000	2
Laverton N GA	Geoscience Australia (2007)	444000	6875000	3
Leinster NW	Barley et al. (2006a, b)	265900	6929400	1
Mount Clifford/Marshall Pool	Beresford et al. (2004)	307803	6848817	2
Mount Keith Cliffs Deposit	Fiorentini (2004)	256950	6982193	1
Mount Keith MKD5 Deposit	Fiorentini (2004)	256333	6987454	1
Mount Keith MKD5 Deposit	Rosengren (2004)	256400	6986800	18
Mount McLure–Bronzewing	Barley et al. (2006a, b)	302811	6969515	1
Mount Monger	Barley et al. (2006a, b)	405473	6563664	16
Mount Weld–Granny Smith	Geoscience Australia (2007)	465000	6803000	9
Mount Windarra	Barley et al. (2006a,b)	427296	6845358	2
Murphy Well	Barley et al. (2006a,b)	423582	6759442	4
Murphy Well east	Barley et al. (2006a, b)	429556	6758178	17
Norseman	Said et al. (2010)	388134	6442071	2
Ora Banda	Barley et al. (2006a, b)			1
Perseverance	Barnes et al. (1995)	273233	6922245	3
Perseverance	Duuring et al. (2010)	274000	6922000	14
Quinn Hills	Barley et al. (2006 a,b)	256711	6803619	1
SE Yilgarn GA	Geoscience Australia (2007)	425500	6718500	2
Spring Well	Barley et al. (2006a, b)	319283	6912353	5
Sullivans South	Thébaud et al. (2012)	331027	6819355	1
Wallaby	Barley et al. (2006a, b)	432743	6700802	11
Welcome Well–Woolshed Well	Barley et al. (2006a, b)	367455	6804650	1
Wiluna	Fiorentini (2004)	220896	7054418	1
Wiluna SW	Barley et al. (2006 a,b)	220122	7045535	6
Yandal GA	Geoscience Australia (2007)			18
Yandal N	Barley et al. (2006 a, b)	281560	7043530	8

VOLCANIC ASSEMBLAGES IN THE EAST YILGARN CRATON

The Archean greenstone belts of the east Yilgarn craton have been a testing ground for tectonic models of granite-greenstone terrane evolution for several decades (Archibald et al., 1978; Groves et al., 1984; Campbell and Hill, 1988; Swager et al., 1997). The felsic and intermediate rocks that form the main topic of this paper occur within the two best-studied and most mineral-endowed terranes comprising the western half of the east Yilgarn craton: the Kalgoorlie and Kurnalpi terranes (Fig. 1). In this section, we present an overview of the entire volcanic package, in order to establish a context for the interpretation of the critical andesitic lithologies.

Ultramafic and Mafic Assemblages

The Kalgoorlie terrane is characterized by a belt of highly magnesian, cumulate-dominated

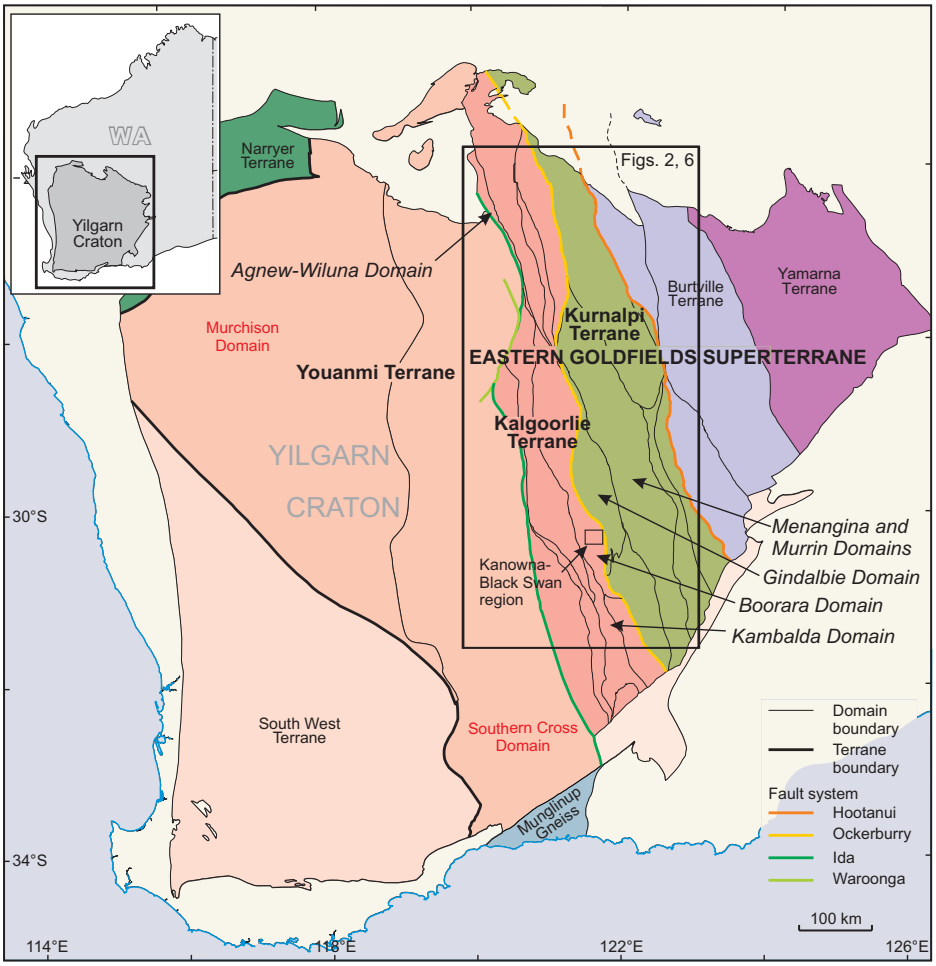

Figure 1. Location map of the Yilgarn craton, modified from Cassidy et al. (2006) showing terrane and domain boundaries, major terrane-bounding faults, locations mentioned in the text, and outline of detailed study area shown in Figure 6.

komatiites and associated contaminated komatiitic basalts that extends from Widgiemooltha in the south to Wiluna in the north, over a strike length of more than 500 km (Fig. 1), and these rocks were erupted over a restricted time period between 2708 and 2690 Ma (Hill et al., 1995; Nelson, 1997; Barnes and Fiorentini, 2012; Fiorentini et al., 2012). The Kalgoorlie terrane komatiites host the world's third largest province of nickel sulfide ore deposits, after Sudbury and Noril'sk-Talnakh, and they account for more than half of the total global endowment of komatiite-hosted nickel sulfide mineralization in a number of camps, of which the major camps are Kambalda, Perseverance, and Mount Keith (Barnes and Fiorentini, 2012). This belt is overwhelmingly the largest (by contained metal tonnes) nickel sulfide province associated with Archean komatiites. Further to the east across the Kurnalpi terrane, komatiites are widespread but are marked by more-evolved, lower-MgO compositions, and a prevalence of compound spinifex-textured flows interpreted as the distal flanks of the major flow fields (Hill et al., 1995). A feature associated with the komatiitic sequence in both terranes is a widespread and very homogeneous unit of low-Th tholeiitic basalts, having geochemical characteristics typical of Archean greenstone belt tholeiites worldwide and bearing strong similarities to Phanerozoic ocean plateau tholeiites (Barnes et al., 2012). The basalt package also includes moderately light rare earth element (LREE)–enriched intermediate-Th tholeiites, and a suite of siliceous high-Mg basalts with strong Th and LREE enrichment interpreted variously as crustally contaminated komatiite (Arndt and Jenner, 1986; Sun, 1989; Lesher and Arndt, 1995) or as products of a strongly heterogeneous mantle plume source (Said and Kerrich, 2009; Said et al., 2012).

The north-south–striking komatiite trend in the Kalgoorlie terrane is interpreted to represent the locus of maximum eruption rate of the hottest komatiite magmas (Barnes and Fiorentini, 2012). The basalt-komatiite assemblage across both terranes, including units intercalated with andesites, has overwhelmingly plume-like characteristics and shows none of the diagnostic characteristics, such as Nb depletion and low Ni, Cr, and Fe contents, of Phanerozoic arc basalts (Barnes et al., 2012). The entire package of komatiites and basalts in the age grouping around 2700 Ma has many of the hallmarks of a large igneous province (Barnes et al., 2012; Ernst, 2007).

Felsic and Intermediate Volcanic Assemblages and Relationship to Komatiites and Basalts

Volcanic and volcaniclastic rocks of andesitic to dacitic affinity are widespread across the Kalgoorlie and Kurnalpi terranes, and much of the assemblage falls within the same age range as the komatiite-basalt assemblage, as indicated in the age-lithostratigraphic chart in Figure 2 after Blewett et al. (2010) and Czarnota et al. (2010). Most of these rocks, as with the basalts and komatiites, have undergone low- to medium-grade regional metamorphism and destruction of primary mineralogy, but with widespread preservation of primary volcanic textures. Rocks of andesite to dacite composition range from lavas to agglomerates and tuffs and are commonly mildly amygdaloidal and porphyritic with up to 25% phenocryst plagioclase (Barley et al., 2006b, 2008). Andesites underlie and overlie low-Th tholeiites and komatiites in the Kurnalpi terrane, spanning an age range from 2720 to 2695 Ma (Blewett et al., 2010; Czarnota et al., 2010), although it is not clear whether the older ages may be due to a component of inherited xenocrysts. Felsic volcanism of dacite to rhyolite composition continued to 2690 Ma (Barley et al., 2008).

Within the Kalgoorlie terrane, komatiites occur in two distinctly different stratigraphic associations. In the Kambalda Domain in the southwest part of the terrane (Fig. 1), komatiites form part of a plume-derived basalt-dominated stratigraphy, underlain by low-Th tholeiites and overlain by intermediate-Th tholeiites and siliceous high-Mg basalts, with little or no felsic material (Fig. 2). Elsewhere in the Kalgoorlie terrane, in the Boorara Domain to the east of Kalgoorlie in the south and in the Agnew-Wiluna Domain in the north (Figs. 1 and 2), dacite flows and tuffs are intimately intercalated with komatiites. In the Kanowna–Black Swan region in the Boorara Domain (Fig. 1), the two magma types appear to have been erupted simultaneously in a spectacular example of bimodal komatiite-dacite volcanism, forming complex peperite mingling textures (Fig. 3A) and invasive pillow-like flow lobes of komatiite

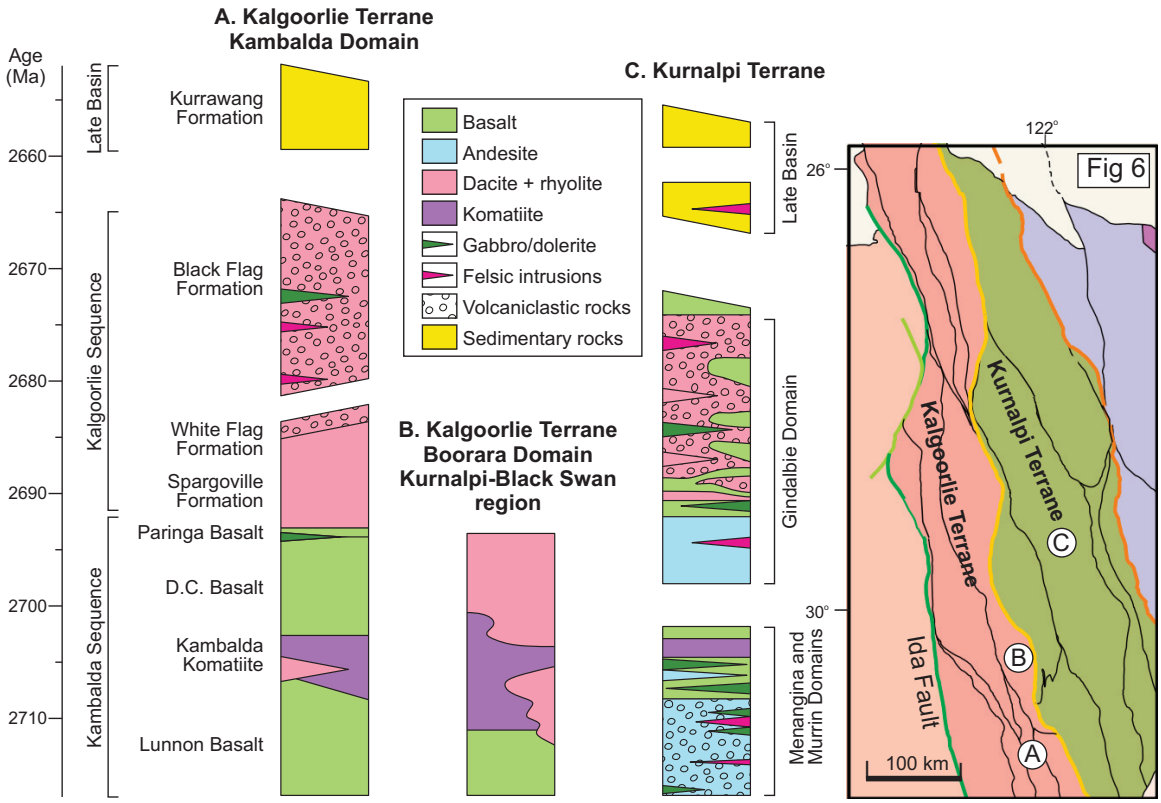

Figure 2. Stratigraphic columns showing timing relationships among mafic, ultramafic, felsic, and intermediate components of the east Yilgarn craton volcanic sequence in the (A) southwestern Kalgoorlie terrane (Kalgoorlie-Kambalda), (B) Black Swan region of the Kalgoorlie terrane (see Fig. 1 for location), and (C) Menangina-Murrin Domains of the Kurnalpi terrane (modified from Czarnota et al., 2010).

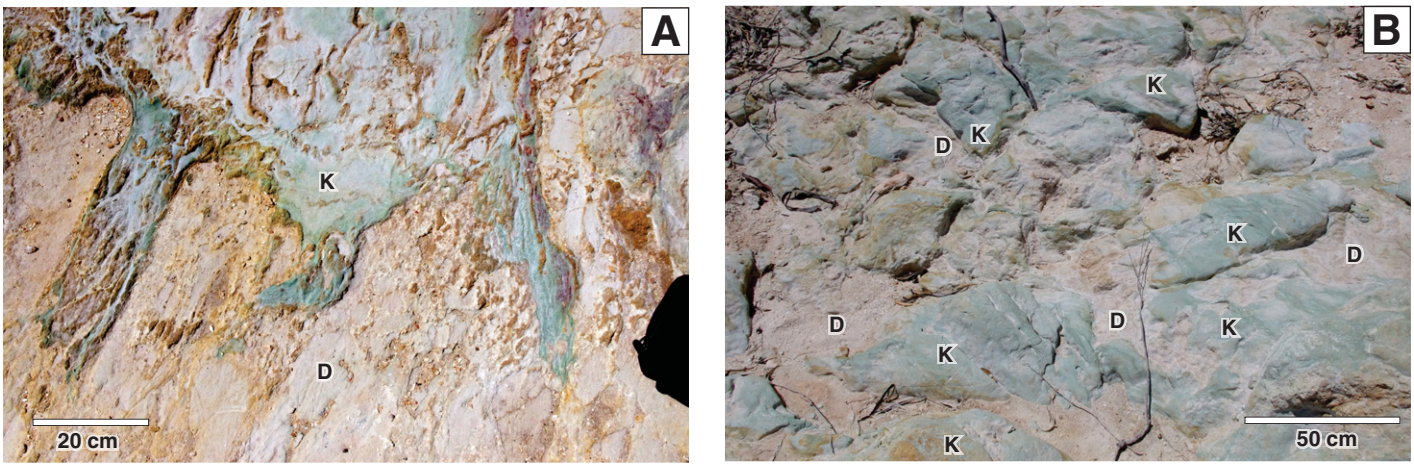

Figure 3. Komatiite-dacite relationships in olistostrome blocks at the Breakaway locality 50 km northeast of Kalgoorlie. (A) Complex "peperite" interfingering of weathered komatiite (green) with dacite ("D," white), interpreted to have been partially consolidated volcaniclastic sediment. (B) Bulbous pillow-like masses of fine-grained weathered komatiite ("K," green) within fine-grained weathered dacitic material, probably ash; plane of bedding approximately parallel to outcrop surface.

(Fig. 3B) injected into soft or partially molten dacite (Trofimovs et al., 2004). Complex intercalations of komatiite and felsic tuffs and lavas are also inferred from closely spaced diamond drill sections through the Black Swan nickel deposit 70 km northeast of Kalgoorlie (Hill et al., 2004). A similar intercalation of co-erupted komatiite and dacite is found within the Agnew-Wiluna Domain in the northern part of the terrane (Duuring et al., 2012; Fiorentini et al., 2012); this region hosts the bulk of the known nickel sulfide mineralization.

These two distinct stratigraphic associations—komatiite + siliceous high-Mg basalt, and komatiite + coeval dacite—are mutually exclusive up and down the terrane. Whereas occasional siliceous high-Mg basalt–like samples are found within the komatiite-dacite associations (as at Black Swan), they are clearly the result of local supracrustal magma mingling, peperite formation (Fig. 3), and within-flow contamination. Thick sequences of siliceous high-Mg basalt lavas are not found in the komatiite-dacite domains, and felsic volcanism (other than the overlying and significantly younger Black Flag rocks) is not found in the komatiite + siliceous high-Mg basalt domains.

Current Tectonic Interpretations

An expanding body of isotopic data, going back to early recognition of anomalous Nd/Sm systematics and old inherited zircons in komatiites at Kambalda (Compston et al., 1986; Claoué-Long et al., 1988), and currently being extended by detailed Pb, Lu-Hf, and Nd-Sm crustal mapping (Champion and Cassidy, 2007; Huston and Blewett, 2012; Wyche et al., 2012; Mole et al., 2013), further supports the now generally accepted view that these komatiites erupted through preexisting continental crust. It is now recognized that the linear belt of high-flux komatiites is spatially related to the edge of the Youanmi terrane "archon," a block of older cratonized crust to the west that has been delineated by the isotopic signal of source rocks to the granitoids (Champion and Cassidy, 2007). This craton-margin relationship, common to many of the world's major nickel sulfide provinces, was attributed by Begg et al. (2010) to emplacement of a mantle plume under the Youanmi archon, and consequent localization of flow of the plume head to give rise to maximum degrees of melting and channelizing of melt products beneath the thinner and more juvenile lithosphere around the edges.

The currently prevalent view of the 2.71–2.69 Ga volcanic rocks of the east Yilgarn craton asserts a distinct difference in tectonic setting between the Kalgoorlie and Kurnalpi terranes. The eastern part (the Kurnalpi terrane) is considered to be an accreted island arc, containing a prevalence of calc-alkaline andesites over TTG dacites, and the western part, the Kalgoorlie terrane, having a higher proportion of TTG dacite to calc-alkaline andesite, is considered to have formed as a back-arc basin (Fig. 1; Barley et al., 2008; Czarnota et al., 2010). The island arc–like character of the andesites in the putative Kurnalpi arc is the pivotal line of evidence for this view (Barley et al., 2006b, 2008; Kositcin et al., 2007; Czarnota et al., 2010).

GEOCHEMISTRY OF THE FELSIC AND INTERMEDIATE VOLCANIC COMPONENT

The felsic and intermediate volcanic rocks of the Kalgoorlie and Kurnalpi terranes span a range of compositions from andesites to soda-rhyolites on the basis of silica and total alkali contents (Fig. 4A). Trace-element characteristics of the felsic and intermediate volcanic rocks span a distinctive range that can be summarized by shapes of rare earth element (REE) patterns (Figs. 4B–4G) and other lithophile immobile trace elements (Figs. 4D–4G). Most of the population falls within, or slightly on the low-Yb side of, the FI-FII categories of Hart et al. (2004).

The population as a whole displays a continuum of REE patterns, incorporating a broad trend of positively correlated La/Sm and Gd/Yb (i.e., light and heavy REE slopes) with a second flat trend toward variable and high Gd/Yb at high but roughly constant La/Sm (Fig. 4C). The higher Gd/Yb character is indicative of an affinity with the TTG suite of magmas, usually interpreted as being moderate- to high-pressure partial melts of mafic precursors in the deep crust (Martin et al., 2005), although they are somewhat less enriched in Th and LREEs and less depleted in Y and Yb than the "type" TTG compositions as defined by Smithies (2000).

A fourfold classification of east Yilgarn craton felsic-intermediate volcanic rocks is proposed (Fig. 4C), based on slopes of the REE patterns: calc-alkaline, low La/Sm; calk-alkaline, having La/Sm_n between 2 and 3.4; TTG, having La/Sm_n greater than 3.4 and Gd/Yb_n mostly greater than 1.5; and TTG, high Gd/Yb, having La/Sm_n greater than 3.4 and Gd/Yb_n greater than ~3, where the subscript n refers to normalization to the primitive mantle composition of McDonough and Sun (1995). The extended trace-element characteristics of these subdivisions are shown in Figures 4D–4G, including Th, Nb, Zr, Ti, and Y with selected rare earth elements. The TTG categories are dominated by dacites and rhyolites and have distinct negative Nb and Ti anomalies (Figs. 4D and 4E). The calk-alkaline categories are dominated by andesites; negative Nb and Ti anomalies are also evident, with the deeper Nb anomalies being associated with the stronger LREE enrichment (Figs. 4F and 4G).

Lithophile trace-element concentrations in east Yilgarn craton andesites closely match Phanerozoic calc-alkaline island-arc andesites (Fig. 5), whereas the associated dacites and rhyolites have distinctly steeper patterns, higher ratios of middle REEs to heavy REEs (as represented by Gd/Yb ratios), and smaller negative Nb and Ti anomalies compared with east Yilgarn craton andesites and with modern arc dacites and rhyolites.

The proposed classification scheme is used to map out the distribution of 2705–2690 Ma felsic and intermediate rocks by geochemical type across the Kalgoorlie and Kurnalpi terranes (Fig. 6). (For convenience in subsequent discussion, we consider the dacite and rhyolite population together and refer to them as dacites.) Geochemical types of dacite are distributed without any obvious spatial control across both the Kalgoorlie and Kurnalpi terranes, although proportionately higher numbers of the TTG types are found within the Kalgoorlie terrane. The andesite groupings are predominantly, although not exclusively, found within the Kurnalpi terrane, with no systematic north-south variation or systematic variability between andesite localities. The TTG type andesites are rare and restricted to the Kalgoorlie terrane, and the low-La/Sm variety is restricted to the northern part of this terrane. In summary, the various dacite types can be found anywhere across the two terranes, but andesites of calc-alkaline type become dominant toward the east. This spatial distribution is key to understanding the tectonic setting.

Geochemical Trends within the Basalt-Andesite-Felsic Array

Figure 7 shows major- and trace-element data for the array of 2710–2690 Ma volcanic rocks of the Kalgoorlie and Kurnalpi terranes, combining the andesite and dacite population with data for the predominant basalt suite, the low-Th tholeiite suite, which extends across both terranes. The entire data set extends almost continuously from highly magnesian komatiites (excluded from the plots for clarity) to highly siliceous rhyolites (Fig. 7). The Kurnalpi terrane andesites are broken out as a combined geographical-geochemical group to test the hypothesis that these rocks represent a distinct island-arc–related component.

The Kurnalpi terrane andesites occupy a position at the high-Si end of the basalt data array (Fig. 7A), chemically intermediate in almost all respects between the tholeiitic basalts

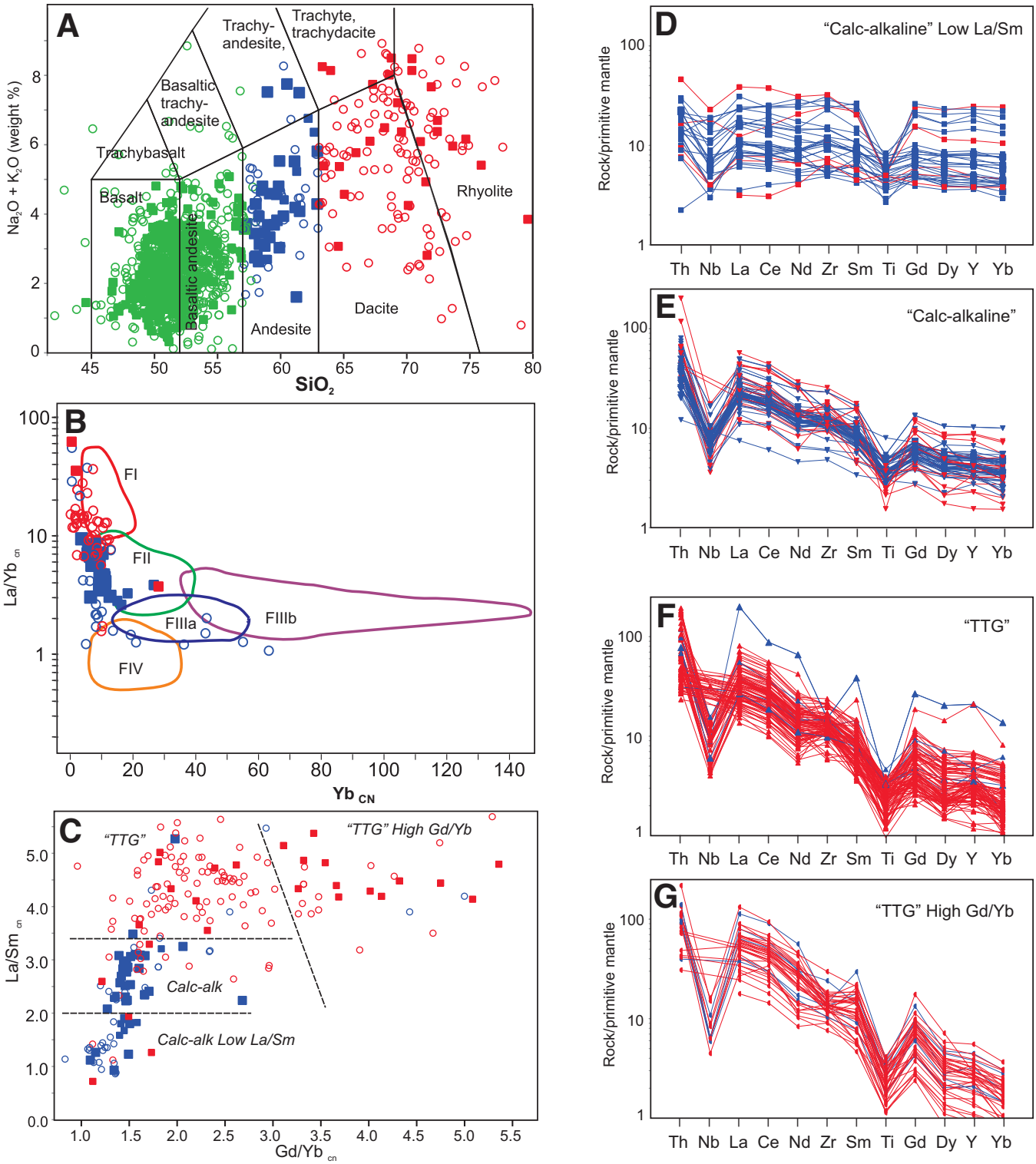

Figure 4. Major- and trace-element classification schemes for intermediate to felsic rocks. (A) Total alkali–silica plot after Le Bas et al. (1986) modified to give threefold classification into basalt, andesite, and dacite-rhyolite groupings. Open circles: Kalgoorlie Terrane; closed squares: Kurnalpi Terrane. (B) Rare earth element (REE)–based FI–FIII classification scheme derived for Abitibi felsic volcanic rocks by Hart et al. (2004). (C) Classification scheme used in this paper based on slopes of heavy and light rare earth element patterns. (D–G) Multi-element spidergrams for the groupings defined in C. TTG—tonalite-trondhjemite-granodiorite.

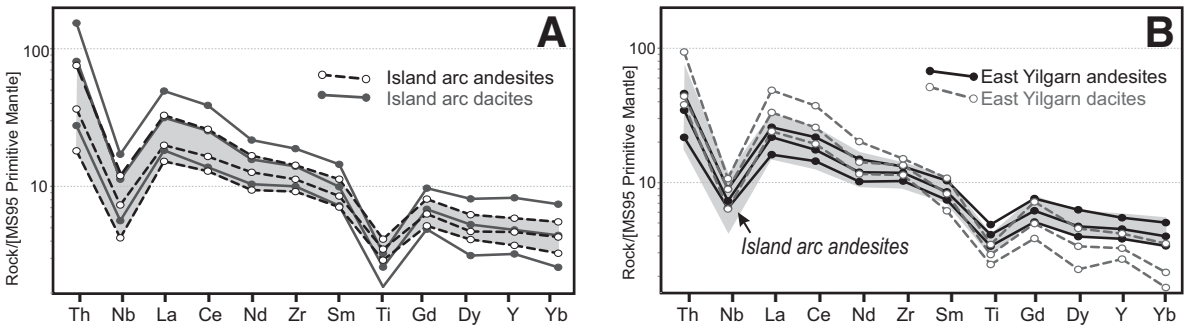

Figure 5. (A) Rare earth element (REE)–high field strength element (HFSE) spidergrams for andesites (593 samples) and dacites (413 samples) from Phanerozoic island arcs. (B) Andesites and dacites from the Kalgoorlie and Kurnalpi terranes of the east Yilgarn craton, superimposed on field for Phanerozoic island-arc andesites (gray shade). Each case shows 25th percentile, 75th percentile, and median values, normalized to McDonough and Sun (1995) primitive mantle (MS95).

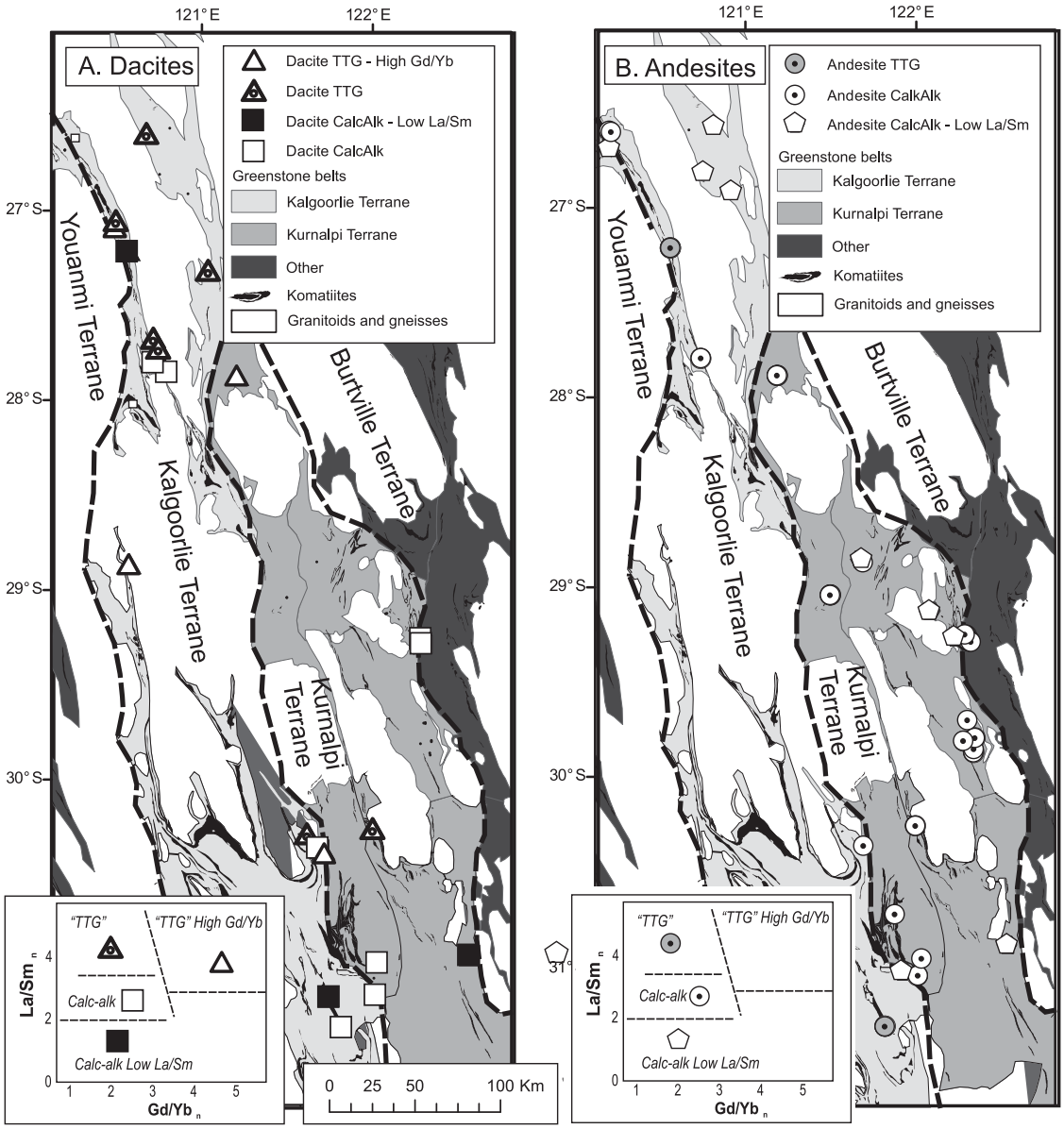

Figure 6. Detailed map showing distribution of komatiites, and felsic (A) and intermediate (B) volcanic rocks across the Kalgoorlie and Kurnalpi terranes, subdivided according to rare earth element characteristics defined in Figure 4C. TTG—tonalite-trondhjemite-granodiorite affinity.

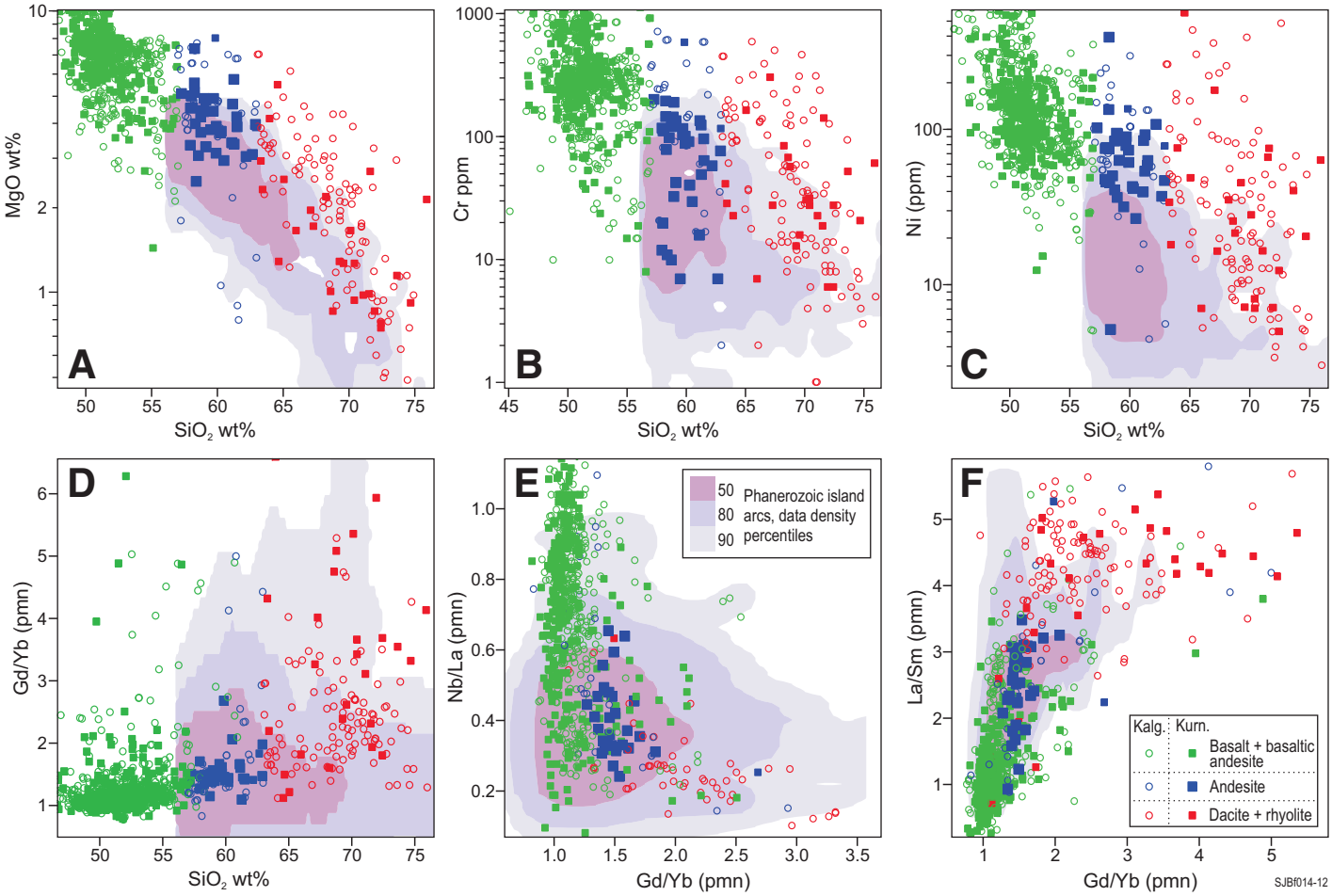

Figure 7. Compilation of geochemical data (recalculated to 100% volatile free) for all volcanic rocks excluding komatiites, for samples dated between 2710 and 2690 Ma from the Kalgoorlie (circles) and Kurnalpi (squares) terranes of the east Yilgarn craton. Background contours show 50th and 80th data density contours on GEOROC data from Phanerozoic island arcs, for intermediate (>56% SiO_2) to felsic volcanic rocks only.

and the main population of dacites. Whereas the andesite grouping is almost exactly coincident with the main mode of modern island-arc data with respect to lithophile incompatible trace elements (Fig. 5, Figs. 7 D–F), they are systematically at, or beyond, the high end of the range of MgO, Ni, and Cr for given values of SiO_2 (Figs. 7A–7C). They are also mildly enriched in Fe and depleted in Al relative to the main data clusters for Phanerozoic arc magmas.

PETROGENETIC MODELING

Two types of quantitative petrogenetic models were tested with a view to reproducing the major- and trace-element geochemistry of the Kurnalpi terrane andesites. The first consists of simple linear mixing of end-member magmas, disregarding phase equilibria and crystallization. Such models (Bédard et al., 2013) are useful in establishing trajectories of incompatible trace-element trends, but they cannot reliably be used to test major-element matches owing to the likelihood of crystallization during mixing.

The second approach allows for simultaneous assimilation and crystallization, using the program PELE (Boudreau, 1999), an implementation of the MELTS thermodynamic simulation of silicate melt equilibria (Ghiorso and Sack, 1995). End-member compositions are listed in Table 2. Hypothetical melt compositions were generated by models involving between 40% and 60% mixing of TTG melt with tholeiite or komatiite magma, combined with between 20% and 40% crystallization of the mixture to produce solid assemblages composed of olivine, orthopyroxene, clinopyroxene, and plagioclase at pressures anywhere from 1 to 10 kbar.

Models involving komatiite failed to reproduce andesite compositions under reasonable sets of assumptions, generating excessive enrichment in lithophile incompatible elements for appropriate MgO and SiO_2. However, contamination of komatiite with TTG dacite, with simultaneous olivine crystallization, gives a close match to the siliceous high-Mg basalts (high-Th basalt suite) exemplified by the Paringa Basalt in the Kalgoorlie terrane, consistent with their previous interpretation as contaminated komatiites (Arndt and Jenner, 1985; Sun et al., 1989; Lesher and Arndt, 1990; Barnes et al., 2012).

Models involving mixing of typical east Yilgarn low-Th tholeiite compositions (with 7.5% MgO as the high-temperature end member), derived from shallow melting of the plume head, and a range of TTG-like contaminants gave excellent matches to the range of Kurnalpi andesite compositions (Figs. 8 and 9). The closest matching results were obtained using a felsic end member having the median composition of dacites erupted in association with komatiites at Black Swan and Perseverance. Magma compositions very similar to Kurnalpi andesites (in REE, Th, Nb, Zr, and Y, in most major and minor elements, and in Ni) are generated by

TABLE 2. INPUT PARAMETERS AND "TARGET" ANDESITE COMPOSITIONS USED IN PELE MODELING

	Median Lunnon-type basalt	Average Perseverance–Black Swan dacite	Median high-Gd/Yb dacite	Kurnalpi andesite median	Kurnalpi andesite 2× std deviation
SiO_2	51.0	71.0	69.2	59.0	3.7
TiO_2	1.0	0.4	0.6	1.0	0.6
Al_2O_3	15.0	15.1	15.9	16.3	2.0
FeO	10.5	2.5	3.0	6.5	4.2
MgO	7.5	1.2	2.2	4.0	1.2
CaO	11.5	2.7	2.4	7.3	3.2
Na_2O	2.0	4.6	4.5	3.4	2.5
K_2O	0.2	1.9	2.0	0.5	1.1
Th	0.3	5.3	8.4	2.5	2.2
Nb	2.5	5.3	4.6	5.1	2.3
La	2.6	23.4	39.7	15.2	44.3
Ce	7.5	44.6	79.4	31.3	49.8
Nd	6.0	18.8	35.0	16.1	31.3
Zr	48	153	152	132	49
Sm	1.9	3.3	5.6	3.8	8.0
Eu	1.0	1.2	1.6	1.2	2.5
Gd	2.6	3.5	4.0	3.9	9.2
Tb		0.5	0.4	0.6	1.5
Dy	3.2	2.4	2.3	3.8	10.4
Y	20.0	14.7	11.9	22.4	80.0
Er		1.4	1.0	2.3	6.6
Yb	2.1	1.3	0.9	2.2	5.8
Cr	300	17	35	99	120
Ni	140	9	29	63	65

Note: Oxides are in weight percent; all other elements are in parts per million.

models involving between 40% and 60% mixing of TTG melt and low-Th tholeiite, combined with between 20% and 40% crystallization of the mixture to produce assemblages of olivine, orthopyroxene, clinopyroxene, and plagioclase at pressures anywhere from 1 to 10 kbar (Fig. 8). Mismatches were observed for Al_2O_3 at low pressures, under which conditions plagioclase is on the liquidus of the mixture. Natural andesites have higher Al_2O_3 by ~2–4 wt% than the model mixtures; however, this anomaly disappears in the 5–10 kbar simulations, where plagioclase crystallization is suppressed, and the mixtures become Al enriched during crystallization. The mismatch in Al_2O_3 may be enhanced by the presence of an accumulated plagioclase phenocryst component in the natural andesites, but the absence of positive Eu anomalies tends to favor an explanation in terms of higher pressures.

The other main mismatch is in Cr, but the Cr content of the model liquids is very highly dependent on whether chromite crystallizes from the mixture. Simulations where chromite is allowed as a liquidus phase tend to give model Cr values that are too low, whereas models without chromite give high Cr values in the appropriate major-element composition range (Fig. 8C). This discrepancy can be attributed to the uncertainties surrounding spinel equilibria in the underlying MELTS model, and uncertainty in knowledge of appropriate oxygen fugacities.

These discrepancies aside, the distinctive calk-alkaline–like trace-element characteristics of the Kurnalpi terrane andesites can be explained entirely by a model involving mantle-plume–derived and crust-derived melts. The proposed model also accounts for the distinctive, anomalously high Ni, Cr, and Mg contents of the east Yilgarn craton andesites.

Isotopic Constraints

A Lu-Hf whole-rock and Lu-Hf zircon isotopic database is gradually accumulating for the volcanic rocks of the Kalgoorlie and Kurnalpi terranes, but not enough coherent data currently exist in the way of multiple isotope systems on individual samples to be able to constrain mixing models with any rigor. Nevertheless, some general statements can be made. Zircons with crystallization ages around 2700 Ma from Kurnalpi terrane andesites are reported as having ε_{Hf} values between +2 and +6, and whole-rock values are between –0.3 and +2 (10 samples: Barley et al., 2003). These values fall between chondritic and mildly depleted in terms of source characteristics. Small numbers of TTG-type dacites from the Kurnalpi terrane are reported by the same authors as having ε_{Hf} between −1.5 and +1.4, also implying sources with Hf isotopic characteristics close to, but more depleted than, calculated values for chondritic mantle (chondritic uniform reservoir [CHUR]). Low-Th basalts from the Kalgoorlie terrane are reported as having ε_{Nd} values predominantly between +1 and +3 (Said et al, 2010), i.e., mildly depleted but also close to chondritic values. Although yet to be comprehensively tested, these data are consistent with derivation of andesite from an essentially primitive, near-chondritic end-member basalt, and a TTG-like dacite with CHUR-like to slightly depleted isotopic characteristics, as implied by the major- and trace-element chemistry presented here.

DISCUSSION

The debate regarding the tectonic setting of east Yilgarn volcanic rocks centers on the question of whether subduction is necessary for the origin of the andesites and specifically the TTG component required for their formation according to the model proposed here. Advocates of plate-driven subduction-accretion models claim an affinity between Archean TTG magmas and modern adakites, believed to have formed by slab melting (Rapp et al., 2003); others have demonstrated that Archean TTGs, with characteristics very similar to the array of compositions seen in the east Yilgarn craton, can be derived by partial melting at the base of thickened crust of underplated mafic rocks with compositions similar to modern oceanic plateau basalts (Smithies, 2000; Bédard, 2006; Smithies et al., 2009; Karsli et al., 2010; Bédard et al., 2013). The evidence from TTG-like magmas on Iceland (Hegner et al., 2007; Willbold et al., 2009) shows that such melts can be derived by partial melting at the base of thick accumulations of plume-derived basalts. This process is likely to have occurred readily in Archean granite-greenstone terranes where komatiites formed a major component of the plume volcanism. The temperature and fluid dynamic properties of komatiites are such that they are capable of generating extensive roof melting above sills, even in the absence of a volatile component, and this may account for the observed bimodal komatiite-dacite volcanism (Huppert and Sparks, 1988) with no assumptions about subduction-related hydration.

A characteristic feature of Archean greenstone belts is a transition from mafic-ultramafic plume-derived magmatism, through andesites, to dacites and rhyolites. Long ascribed to convergent margin settings, this juxtaposition of extensive plume-head magmatism with calk-alkaline intermediate to felsic volcanic rocks poses a major problem for geotectonic interpretations of Archean crustal growth. Data and calculations presented here provide an alternative explanation for the origin of Archean andesites within such evolving successions, through mix-

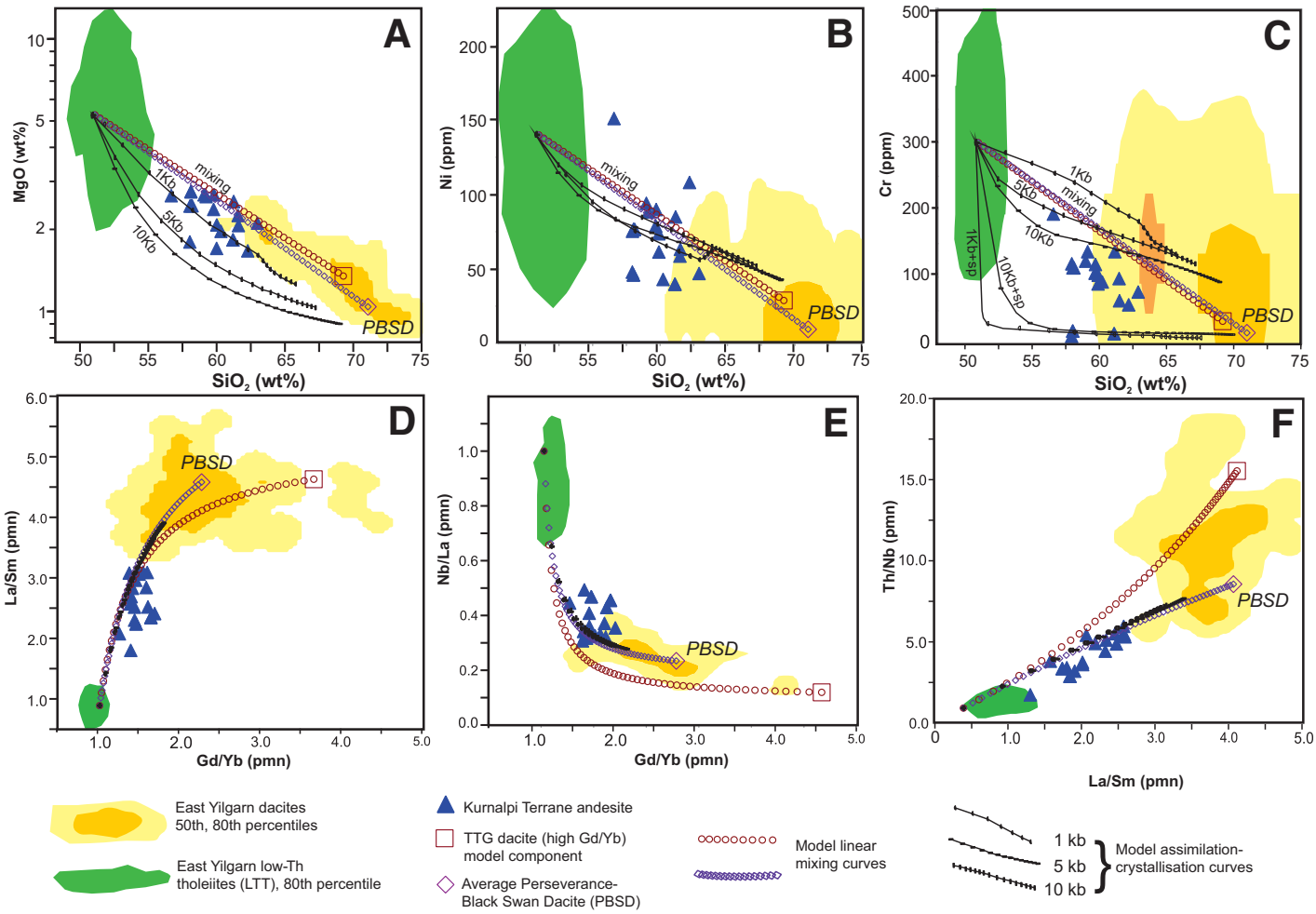

Figure 8. Examples of linear mixing models (open symbols) and "MELTS"-based assimilation-equilibrium crystallization models (black symbols) for starting material with median composition of a low-Th tholeiite (LTT) basalt with average Perseverance and Black Swan dacite and median high-Gd/Yb tonalite-trondhjemite-granodiorite (TTG)–type Kalgoorlie terrane dacite. Pressure in kilobars is indicated on model curve legend. Model crystallization-assimilation curves are virtually coincident on the ratio-ratio plots. Abbreviations are explained in the legend. PBSD—Perseverance–Black Swan dacite.

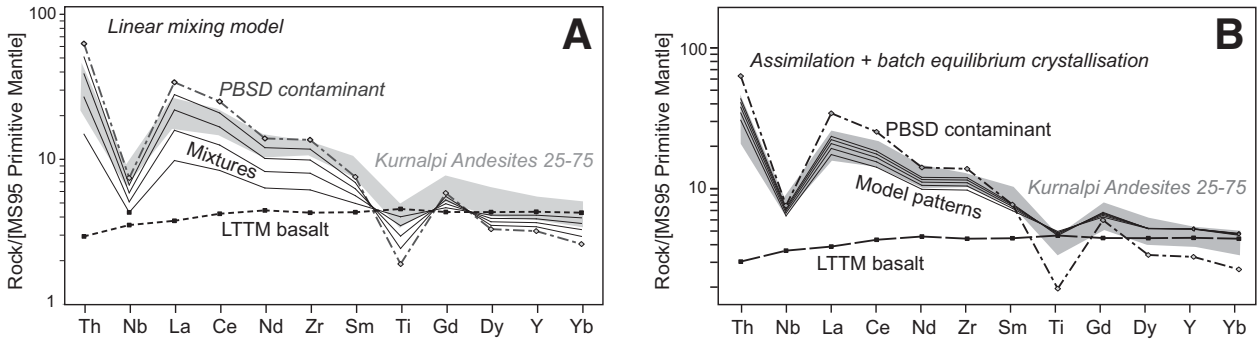

Figure 9. Result of mixing and assimilation-crystallization models for basalt-dacite end members plotted on multi-element spidergrams, with normalization to primitive mantle of McDonough and Sun (1995) (MS95). (A) Simple linear mixing model. (B) Assimilation-batch equilibrium crystallization model, 3 kbar pressure, median low-Th tholeiite (LTTM) contaminated with median Perseverance–Black Swan dacite (PBSD) composition. Model patterns are shown for synthetic compositions with 59%–62% SiO_2, 47%–58% crystallized, 70%–100% assimilant added (relative to 100% starting mafic magma).

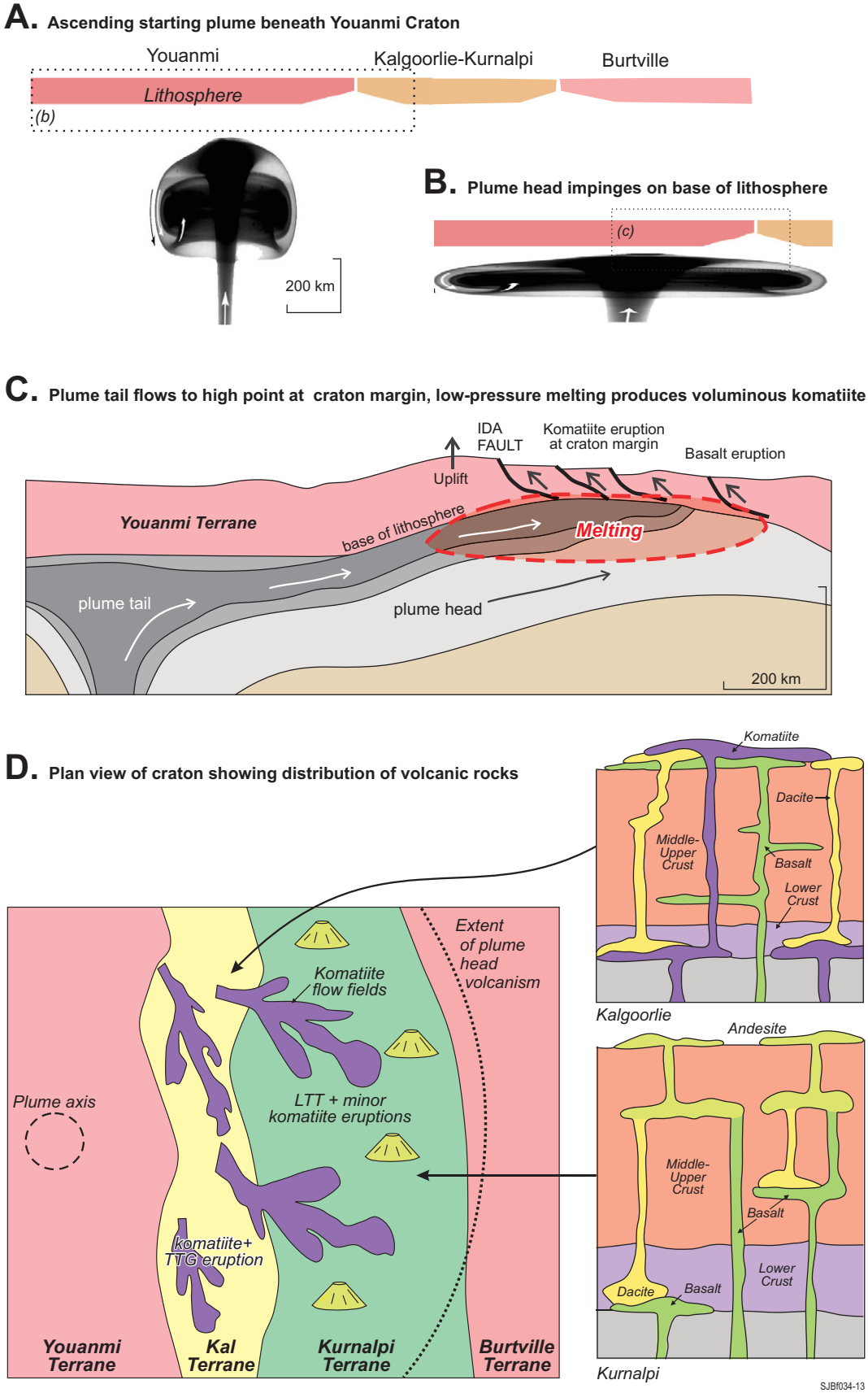

Figure 10. Tectonic model for development of the east Yilgarn craton large igneous province showing proposed relationship of komatiites, basalts, tonalite-trondhjemite-granodiorite (TTG) dacites, and andesites, modified from Barnes et al. (2012). (A) Starting plume ascending beneath the Youanmi archon, within a few hundred kilometers of an original boundary with more juvenile proto–Eastern Goldfields craton. Plume head is mixture of high-temperature tail (generating komatiite melts) and entrained ambient mantle (Campbell et al., 1989; Griffiths and Campbell, 1990). (B) Impingement and flattening of plume head beneath lithosphere. (C) Channeling of plume head and tail to thinnest lithosphere at craton margin, generation of continental rifting centered on original suture, and onset of komatiite and low-Th basalt production. Maximum melt production occurs beneath Youanmi craton margin, controlled by flow of plume along sloping base of craton margin (Begg et al., 2010), focusing of predominant flux of komatiite plume-tail melt at craton margin. (D) Plan view of time frame in C with widespread eruption of komatiite, low-Th tholeiite (LTT), and associated TTG crustal melt products along Kalgoorlie (Kal) terrane, controlled by presence of inherited through-going translithospheric structures. High magma flux results in extensive melting of underplated mafic crustal material and co-eruption of komatiite and TTG dacite. Further east, low-Th tholeiite and less-voluminous komatiite eruptions extend ~1000 km east of original plume axis; distal komatiite facies also form in extensive komatiite flow fields originating in or near the Kalgoorlie terrane. Mixing of tholeiite with TTG dacite and rhyolites generated in lower and midcrust generates a spectrum of andesitic magmas processed through midcrustal magma chambers.

ing of plume-derived basalts and TTG-like magmas derived from melting of preexisting mafic crust, probably consisting of a major component of underplated plume-derived basalt, entirely within a plume-driven tectonic setting. In this model, we regard the TTG-like dacite suite as being analogous to Icelandic dacites generated by deep melting within a thick basaltic pile (Hegner et al., 2007; Smithies et al., 2009; Willbold et al., 2009).

As noted already, the komatiite-basalt volcanic suite considered here is characterized by voluminous eruption of plume-related mafic and ultramafic volcanic rocks over a restricted time period; these are the essential attributes of a large igneous province (Richards et al., 1989; Eldholm and Coffin, 2000; Ernst, 2007). In this case, large igneous province magmatism involved extensive melting of preexisting continental crust, as evidenced by the bimodal komatiite-dacite assemblages described herein. Andesites are generated in the more distal portions of the province, where the flux of magma through preexisting continental crust is dominated by tholeiitic basalt derived from the plume head, rather than by komatiites derived from the plume tail (Fig. 10; Campbell et al., 1989). This model accounts for the absence of island-arc signatures in associated basalts and has significant implications for the interpretation of Archean tectonics.

The evidence presented here suggests caution in concluding a priori that the presence of calc-alkaline andesites in greenstone belts necessarily implies subduction. Plume-crust interaction, rather than plume-arc interaction, provides a much simpler explanation for the tectonic and stratigraphic evolution of the east Yilgarn craton lithosphere, and potentially for other typical Archean greenstone belts.

ACKNOWLEDGMENTS

We thank Steve Hollis, John Walshe, and Bill Collins for helpful reviews of early versions, and Jean Bedard, Ian Campbell, an anonymous reviewer, and Science Editor John Goodge for formal reviews that greatly improved the manuscript. Travis Naughton (Commonwealth Scientific and Industrial Research Organisation [CSIRO]) drafted the figures. This work is an output of the CSIRO Minerals Down Under National Research Flagship, and Barnes acknowledges funding from that source. Van Kranendonk acknowledges funding support from the University of New South Wales. This is publication 395 of the Australian Research Council Centre of Excellence for Core to Crust Fluid Systems.

REFERENCES CITED

Archibald, N.J., Bettenay, L.F., Binns, R.A., Groves, D.I., and Gunthorpe, R.J., 1978, The evolution of Archean greenstone terrains, Eastern Goldfields Province, Western Australia: Precambrian Research, v. 6, p. 103–131, doi:10.1016/0301-9268(78)90008-6.

Arndt, N.T., and Jenner, G.A., 1985, Kambalda komatiites and basalts: Evidence for subduction of sediments in the Archaean mantle: Terra Cognita, v. 5, p. 206.

Arndt, N.T., and Jenner, G.A., 1986, Crustally contaminated komatiites and basalts from Kambalda, Western Australia: Chemical Geology, v. 56, p. 229–255, doi:10.1016/0009-2541(86)90006-9.

Ayer, J., Amelin, Y., Corfu, F., Kamo, S., Ketchum, J., Kwok, K., and Trowell, N., 2002, Evolution of the southern Abitibi greenstone belt based on U-Pb geochronology: Autochthonous volcanic construction followed by plutonism, regional deformation and sedimentation: Precambrian Research, v. 115, p. 63–95, doi:10.1016/S0301-9268(02)00006-2.

Barley, M.E., Blewett, R.S., Cassidy, K.F., Champion, D.C., Czarnota, K., Doyle, M.G., Krapež, B., Kositcin, N., Pickard, A.L., and Weinburg, F., 2006a, Tectonostratigraphic and Structural Architecture of the East Yilgarn Craton: Australian Minerals Industry Association Report P763/pmd*CRC Project Y1.

Barley, M.E., Brown, S.J.A., and Krapez, B., 2006b, Felsic volcanism in the eastern Yilgarn craton, Western Australia: Evolution of a late Archean convergent margin: Geochimica et Cosmochimica Acta, v. 70, p. A35, doi:10.1016/j.gca.2006.06.178.

Barley, M.E., Krapez, S., and Kositcin, N., 2008, Physical volcanology and geochemistry of a late Archaean volcanic arc, Kurnalpi and Gindalbie terranes, Eastern Goldfields superterrane, Western Australia: Precambrian Research, v. 161, p. 53–76, doi:10.1016/j.precamres.2007.06.019.

Barnes, S.J., and Fiorentini, M.L., 2012, Komatiite magmas and nickel sulfide deposits: A comparison of variably endowed Archean terranes: Economic Geology and the Bulletin of the Society of Economic Geologists, v. 107, p. 755–780, doi:10.2113/econgeo.107.5.755.

Barnes, S.J., Lesher, C.M., and Keays, R.R., 1995, Geochemistry of mineralised and barren komatiites from the Perseverance nickel deposit, Western Australia: Lithos, v. 34, p. 209–234, doi:10.1016/0024-4937(95)90023-3.

Barnes, S.J., Van Kranendonk, M.J., and Sonntag, I., 2012, Geochemistry and tectonic setting of basalts from the Eastern Goldfields superterrane: Australian Journal of Earth Sciences, v. 59, p. 707–735, doi:10.1080/08120099.2012.687398.

Bédard, J.H., 2006, A catalytic delamination-driven model for coupled genesis of Archaean crust and sub-continental lithospheric mantle: Geochimica et Cosmochimica Acta, v. 70, no. 5, p. 1188–1214, doi:10.1016/j.gca.2005.11.008.

Bédard, J.H., 2013, How many arcs can dance on the head of a plume? A 'Comment' on: "A critical assessment of Neoarchean 'plume only' geodynamics: Evidence from the Superior province," by Derek Wyman: Precambrian Research, v. 229, p. 189–197, doi:10.1016/j.precamres.2012.05.004.

Bédard, J.H., Harris, L.B., and Thurston, P.C., 2013, The hunting of the snArc: Precambrian Research, v. 229, p. 20–48, doi:10.1016/j.precamres.2012.04.001.

Begg, G.C., Hronsky, J.A.M., Arndt, N.T., Griffin, W.L., O'Reilly, S.Y., and Hayward, N., 2010, Lithospheric, cratonic and geodynamic setting of Ni-Cu-PGE sulfide deposits: Economic Geology and the Bulletin of the Society of Economic Geologists, v. 105, p. 1057–1070, doi:10.2113/econgeo.105.6.1057.

Beresford, S.W., Duuring, P., Fiorentini, M.L., Rosengren, N., Bleeker, W., Barley, M., Cas, R., Tait, M., and Wallace, H., 2004, The Structural and Stratigraphic Architecture of the Agnew-Wiluna Belt, Western Australia: AMIRA P710A Final Report: Melbourne, AMIRA.

Blewett, R.S., Czarnota, K., and Henson, P.A., 2010, Structural-event framework for the eastern Yilgarn craton, Western Australia, and its implications for orogenic gold: Precambrian Research, v. 183, p. 203–229, doi:10.1016/j.precamres.2010.04.004.

Boudreau, A.E., 1999, PELE; a version of the MELTS software program for the PC platform: Computers & Geosciences, v. 25, no. 2, p. 201, doi:10.1016/S0098-3004(98)00117-4.

Campbell, I.H., and Hill, R.I., 1988, A two-stage model for the formation of the granite-greenstone terrains of the Kalgoorlie-Norseman area: Earth and Planetary Science Letters, v. 90, p. 11–25, doi:10.1016/0012-821X(88)90107-0.

Campbell, I.H., Griffiths, R.W., and Hill, R.I., 1989, Melting in an Archaean mantle plume: Heads it's basalts, tails it's komatiites: Nature, v. 339, p. 697–699, doi:10.1038/339697a0.

Cassidy, K.F., Champion, D.C., Krapez, B., Barley, M.E., Brown, S.J.A., Blewett, R.S., Groenewald, P.B., and Tyler, I.M., 2006, A Revised Geological Framework for the Yilgarn Craton, Western Australia: Perth, Geological Survey of Western Australia Record 2006/8, 8 p.

Champion, D.C., and Cassidy, K.F., 2007, An overview of the Yilgarn craton and its crustal evolution, *in* Bierlein, F.P., and Knox-Robinson, C.M., eds., Proceedings of Geoconferences (WA) Inc., Kalgoorlie '07 Conference: Geoscience Australia Record, v. 2007, no. 14, p. 8–12.

Claoué-Long, J.C., Compston, W., and Cowden, A., 1988, The age of the Kambalda greenstones resolved by ion-microprobe: Implications for Archaean dating methods: Earth and Planetary Science Letters, v. 89, p. 239–259, doi:10.1016/0012-821X(88)90175-6.

Compston, W., Williams, I.S., Campbell, I.H., and Gresham, J.J., 1986, Zircon xenocrysts from the Kambalda volcanics: Age constraints and direct evidence for older continental crust below the Kambalda-Norseman greenstones: Earth and Planetary Science Letters, v. 76, p. 299–311, doi:10.1016/0012-821X(86)90081-6.

Czarnota, K., Champion, D.C., Goscombe, B., Blewett, R.S., Cassidy, K.F., Henson, P.A., and Groenewald, P.B., 2010, Geodynamics of the eastern Yilgarn craton: Precambrian Research, v. 183, no. 2, p. 175–202, doi:10.1016/j.precamres.2010.08.004.

Duuring, P., Bleeker, W., and Beresford, S.W., 2007, Structural modification of the komatiite-associated Harmony nickel sulfide deposit, Leinster, Western Australia: Economic Geology and the Bulletin of the Society of Economic Geologists, v. 102, p. 277–297, doi:10.2113/gsecongeo.102.2.277.

Duuring, P., Bleeker, W., Beresford, S.W., and Hayward, N., 2010, Towards a volcanic-structural balance: Relative importance of volcanism, folding and remobilisation of nickel sulphides at the Perseverance Ni-Cu-(PGE) deposit: Mineralium Deposita, v. 45, p. 281–311, doi:10.1007/s00126-009-0274-y.

Duuring, P., Bleeker, W., Beresford, S.W., Fiorentini, M.L., and Rosengren, N., 2012, Structural evolution of the Agnew-Wiluna greenstone belt, eastern Yilgarn craton, and implications for komatiite-hosted Ni sulfide exploration: Australian Journal of Earth Sciences, v. 59, p. 765–792, doi:10.1080/08120099.2012.693540.

Eldholm, O., and Coffin, M.F., 2000, Large igneous provinces and plate tectonics, *in* Richards, M., Gordon, R., and Van der Hilst, R., eds., The History and Dynamics of Global Plate Motions: American Geophysical Union Geophysical Monograph 121, p. 309–326.

Ernst, R.E., 2007, Mafic-ultramafic large igneous provinces (LIPs): Importance of the pre-Mesozoic record: Episodes, v. 30, no. 2, p. 108–114.

Fiorentini, M., 2004, PGE Geochemistry of Komatiites, Agnew-Wiluna Belt (WA): Implications for NiS Ore Genesis and Composition of the Archaean Mantle: Crawley, Australia, University of Western Australia, 280 p.

Fiorentini, M.L., Beresford, S.W., Barley, M.E., Duuring, P., Bekker, A., Rosengren, N., Cas, R., and Hronsky, J., 2012, District to camp controls on the genesis of komatiite-hosted nickel sulfide deposits, Agnew-Wiluna greenstone belt, Western Australia: Insights from the multiple sulfur isotopes: Economic Geology and the Bulletin of the Society of Economic Geologists, v. 107, p. 781–796, doi:10.2113/econgeo.107.5.781.

Geoscience Australia (2007) OZCHEM National Whole Rock Geochemistry Database http://www.ga.gov.au/meta/ANZCW0703011055.html

Ghiorso, M.S., and Sack, R.O., 1995, Chemical mass-transfer in magmatic processes. 4. A revised and internally consistent thermodynamic model for the interpolation and extrapolation of liquid-solid equilibria in magmatic systems at elevated temperatures and pressures: Contributions to Mineralogy and Petrology, v. 119, p. 197–212, doi:10.1007/BF00307281.

Griffiths, R.W., and Campbell, I.H., 1990, Stirring and structure in mantle starting plumes: Earth and Planetary Science Letters, v. 99, p. 66–78, doi:10.1016/0012-821X(90)90071-5.

Groves, D.I., Lesher, C.M., and Gee, R.D., 1984, Tectonic setting of the sulphide nickel deposits of the Western Australian Shield, *in* Buchanan, D.L., and Jones, M.J., eds., Sulphide Deposits in Mafic and Ultramafic Rocks: London, Institute of Mining and Metallurgy, p. Jan-13.

Hamilton, W.B., 1998, Archean magmatism and deformation were not products of plate tectonics: Precambrian

Research, v. 91, p. 143–179, doi:10.1016/S0301-9268(98)00042-4.

Hart, T.R., Gibson, H.L., and Lesher, C.M., 2004, Trace element geochemistry and petrogenesis of felsic volcanic rocks associated with volcanogenic massive Cu-Zn-Pb sulfide deposits: Economic Geology and the Bulletin of the Society of Economic Geologists, v. 99, no. 5, p. 1003–1013, doi:10.2113/gsecongeo.99.5.1003.

Hegner, E., Willbold, M., Stracke, A., Rocholl, A., and Anonymous, 2007, Nb-depleted calc-alkaline dacites from Iceland; implications for Archean crust formation: Geochimica et Cosmochimica Acta, v. 71, no. 15s, p. A389.

Hill, R.E.T., Barnes, S.J., Gole, M.J., and Dowling, S.E., 1995, The volcanology of komatiites as deduced from field relationships in the Norseman-Wiluna greenstone belt, Western Australia: Lithos, v. 34, p. 159–188, doi:10.1016/0024-4937(95)90019-5.

Hill, R.E.T., Barnes, S.J., Thordarson, T., Dowling, S.E., and Mattox, T.N., 1999, The Geology of the Black Swan Succession and Associated Nickel Sulfide Orebodies: Commonwealth Scientific and Industrial Research Organisation (CSIRO) Exploration and Mining Report 646R.

Hill, R.E.T., Barnes, S.J., Dowling, S.E., and Thordarson, T., 2004, Komatiites and nickel sulfide ores of the Black Swan area, Yilgarn craton, Western Australia: 1. Petrology and volcanology of host rocks: Mineralium Deposita, v. 39, p. 684–706, doi:10.1007/s00126-004-0437-9.

Hooper, P.R., Binger, G.B., and Lees, K.R., 2002, Ages of the Steens and Columbia River flood basalts and their relationship to extension-related calc-alkalic volcanism in eastern Oregon: Geological Society of America Bulletin, v. 114, p. 43–50, doi:10.1130/0016-7606(2002)114<0043:AOTSAC>2.0.CO;2.

Huppert, H.E., and Sparks, R.S.J., 1988, Melting the roof of a magma chamber containing a hot, turbulently convecting fluid: Journal of Fluid Mechanics, v. 188, p. 107–131, doi:10.1017/S0022112088000655.

Huston, D.L., and Blewett, R.S., 2012, Australia through time; a summary of its tectonic and metallogenic evolution: Episodes, v. 35, no. 1, p. 23.

Karsli, O., Dokuz, A., Uysal, I., Aydin, F., Kandemir, R., and Wijbrans, J., 2010, Generation of Early Cenozoic adakitic volcanism by partial melting of mafic lower crust, eastern Turkey: Implications for crustal thickening to delamination: Lithos, v. 114, p. 109–120, doi:10.1016/j.lithos.2009.08.003.

Kerrich, R., Wyman, D., Fan, J., and Bleeker, W., 1998, Boninite series: Low Ti-tholeiite associations from the 2.7 Ga Abitibi greenstone belt: Earth and Planetary Science Letters, v. 164, p. 303–316, doi:10.1016/S0012-821X(98)00223-4.

Kositcin, N., Brown, S.J.A., Barley, M.E., Krapež, B., Cassidy, K.F., and Champion, D.C., 2007, SHRIMP U-Pb zircon age constraints on the late Archaean tectonostratigraphic architecture of the Eastern Goldfields superterrane, Yilgarn craton, Western Australia: Precambrian Research, v. 161, p. 5–33, doi:10.1016/j.precamres.2007.06.018.

Le Bas, M.J., Le Maitre, R.W., Streckeisen, A., and Zanettin, B., 1986, A chemical classification of volcanic rocks based on the total alkali–silica diagram: Journal of Petrology, v. 27, p. 745–750, doi:10.1093/petrology/27.3.745.

Lesher, C.M., and Arndt, N.T., 1990, Komatiites from Kambalda: Why some are contaminated and others are not [abs.], *in* 7th International Conference on Geochronology, Cosmochronology and Isotope Geology, Abstracts: Geological Society of Australia.

Lesher, C.M., and Arndt, N.T., 1995, REE and Nd isotope geochemistry, petrogenesis and volcanic evolution of contaminated komatiites at Kambalda, Western Australia: Lithos, v. 34, no. 1–3, p. 127–157, doi:10.1016/0024-4937(95)90017-9.

Martin, H., Smithies, R.H., Rapp, R., Moyen, J.-F., and Champion, D., 2005, An overview of adakite, tonalite-trondhjemite-granodiorite (TTG), and sanukitoid; relationships and some implications for crustal evolution: Lithos, v. 79, no. 1–2, p. 1, doi:10.1016/j.lithos.2004.04.048.

McDonough, W.F., and Sun, S.-S., 1995, The composition of the Earth: Chemical Geology, v. 120, p. 223–253, doi:10.1016/0009-2541(94)00140-4.

Mole, D., Fiorentini, M.L., Cassidy, K.F., Kirkland, C.L., Thébaud, N., McCuaig, T.C., Doublier, M.P., Duuring, P., Romano, S., Maas, R., Belousova, E., Barnes, S.J., and Miller, J.M., 2014, Crustal evolution, intra-cratonic architecture and the metallogeny of an Archaean craton, *in* Jenkin, G.R.T., Lusty, P.A.J., McDonald, I., Smith, M.P., Boyce, A.J., and Wilkinson, J.J., eds., Ore Deposits in an Evolving Earth: Geological Society of London Special Publication 393 (in press).

Morris, P. A., and Kirkland, C. L., 2014, Melting of a subduction-modified mantle source: A case study from the Archean Marda Volcanic Complex, central Yilgarn Craton, Western Australia: Lithos, v. 190-191, p. 403–419.

Nelson, D.R., 1997, Evolution of the Archaean granite-greenstone terranes of the Eastern Goldfields, Western Australia: SHRIMP U-Pb zircon constraints: Precambrian Research, v. 83, p. 57–81, doi:10.1016/S0301-9268(97)00005-3.

Rapp, R.P., Shimizu, N., and Norman, M.D., 2003, Growth of early continental crust by partial melting of eclogite: Nature, v. 425, p. 605–609, doi:10.1038/nature02031.

Reubi, O., and Blundy, J., 2009, A dearth of intermediate melts at subduction zone volcanoes and the petrogenesis of arc andesites: Nature, v. 461, p. 1269–1273, doi:10.1038/nature08510.

Richards, M.A., Duncan, R.A., and Courtillot, V.E., 1989, Flood basalts and hotspot tracks; plume heads and tails: Science, v. 246, p. 103–106, doi:10.1126/science.246.4926.103.

Rosengren, N.M., 2004, Architecture and Emplacement Origin of an Archaean Komatiitic Dunite and Associated NiS Mineralisation: Mount Keith, Agnew-Wiluna Greenstone Belt, Yilgarn Craton, Western Australia [Ph.D. thesis]: Melbourne, Australia, Monash University.

Said, N., and Kerrich, R., 2009, Geochemistry of coexisting depleted and enriched Paringa Basalts, in the 2.7 Ga Kalgoorlie terrane, Yilgarn craton, Western Australia; evidence for a heterogeneous mantle plume event: Precambrian Research, v. 174, no. 3–4, p. 287–309, doi:10.1016/j.precamres.2009.08.002.

Said, N., Kerrich, R., and Groves, D., 2010, Geochemical systematics of basalts of the Lower Basalt Unit, 2.7 Ga Kambalda Sequence, Yilgarn craton, Australia; plume impingement at a rifted craton margin: Lithos, v. 115, no. 1–4, p. 82–100, doi:10.1016/j.lithos.2009.11.008.

Said, N., Kerrich, R., Cassidy, K., and Champion, D.C., 2012, Characteristics and geodynamic setting of the 2.7 Ga Yilgarn heterogeneous plume and its interaction with continental lithosphere: Evidence from komatiitic basalt and basalt geochemistry of the Eastern Goldfields superterrane: Australian Journal of Earth Sciences, v. 59, p. 737–764, doi:10.1080/08120099.2012.695294.

Sarbas, B., 2008, The GEOROC database as part of a growing geoinformatics network, *in* Brady, S.R., Sinha, A.K., and Gunderson, L.C., eds., Proceedings Geoinformatics 2008—Data to Knowledge: U.S. Geological Survey Scientific Investigations Report 2008–5172, p. 42–43.

Scarrow, J.H., Molina, J.F., Bea, F., and Montero, P., 2008, Within-plate calc-alkaline rocks: Insights from alkaline mafic magma-peraluminous crustal melt hybrid appinites of the Central Iberian Variscan continental collision: Lithos, v. 110, p. 50–64, doi:10.1016/j.lithos.2008.12.007.

Smithies, R.H., 2000, The Archaean tonalite-trondhjemite-granodiorite (TTG) series is not an analogue of Cenozoic adakite: Earth and Planetary Science Letters, v. 182, no. 1, p. 115, doi:10.1016/S0012-821X(00)00236-3.

Smithies, R.H., Champion, D.C., and Van Kranendonk, M.J., 2007, The oldest well preserved felsic volcanic rocks on Earth; geochemical clues to the early evolution of the Pilbara Supergroup and implications for the growth of a Paleoarchean protocontinent, *in* Van Kranendonk, M.J., Smithies, R.H., and Bennet, V., eds., Earth's Oldest Rocks: Developments in Precambrian Geology 15: Amsterdam, Elsevier, p. 339–367.

Smithies, R.H., Champion, D.C., and Van Kranendonk, M.J., 2009, Formation of Paleoarchean continental crust through infracrustal melting of enriched basalt: Earth and Planetary Science Letters, v. 281, no. 3–4, p. 298, doi:10.1016/j.epsl.2009.03.003.

Sun, S.-S., 1989, Chemical and isotopic composition of Archaean komatiites and siliceous high magnesian basalts: Constraints on early history of Earth and formation of continental crust, *in* 28th International Geological Congress, Abstracts, Volume 3.

Sun, S.-S., Nesbitt, R.W., and McCulloch, M.T., 1989, Geochemistry and petrogenesis of Archaean and early Proterozoic siliceous high-magnesian basalts, *in* Crawford, A.J., ed., Boninites: London, Unwin Hyman, p. 148–173.

Swager, C., and Griffin, T.J., 1990, An early thrust duplex in the Kalgoorlie-Kambalda greenstone belt, Eastern Goldfields Province, Western Australia: Precambrian Research, v. 48, p. 63–73, doi:10.1016/0301-9268(90)90057-W.

Swager, C.P., Goleby, B.R., Drummond, B.J., Rattenbury, M.S., and Williams, P.R., 1997, Crustal structure of granite-greenstone terranes in the Eastern Goldfields, Yilgarn craton, as revealed by seismic reflection profiling: Precambrian Research, v. 83, no. 1–3, p. 43–56, doi:10.1016/S0301-9268(97)00004-1.

Thébaud, N., Barnes, S.J., and Fiorentini, M.L., 2012, Komatiites of the Wildara Leonora belt, Yilgarn craton, WA: The missing link in the Kalgoorlie terrane?: Precambrian Research, v. 196–197, p. 234–246, doi:10.1016/j.precamres.2011.11.008.

Trofimovs, J., Davis, B.K., and Cas, R.A.F., 2004, Contemporaneous ultramafic and felsic intrusive and extrusive magmatism in the Archaean Boorara Domain, Eastern Goldfields superterrane, Western Australia, and its implications: Precambrian Research, v. 131, no. 3–4, p. 283–304, doi:10.1016/j.precamres.2003.12.012.

Willbold, M., Hegner, E., Stracke, A., and Rocholl, A., 2009, Continental geochemical signatures in dacites from Iceland and implications for models of early Archaean crust formation: Earth and Planetary Science Letters, v. 279, no. 1–2, p. 44–52, doi:10.1016/j.epsl.2008.12.029.

Wyche, S., Kirkland, C.L., Riganti, A., Pawley, M.J., Belousova, E., and Wingate, M.T.D., 2012, Isotopic constraints on stratigraphy in the central and eastern Yilgarn craton, Western Australia: Australian Journal of Earth Sciences, v. 59, p. 657–670, doi:10.1080/08120099.2012.697677.

Wyman, D.A., Kerrich, R., and Polat, A., 2002, Assembly of Archean cratonic mantle lithosphere and crust: Plume-arc interaction in the Abitibi-Wawa subduction-accretion complex: Precambrian Research, v. 115, p. 37–62, doi:10.1016/S0301-9268(02)00005-0.

MANUSCRIPT RECEIVED 27 NOVEMBER 2013
REVISED MANUSCRIPT RECEIVED 3 FEBRUARY 2014
MANUSCRIPT ACCEPTED 09 FEBRUARY 2014

Printed in the USA